An Anthropomorphic Phantom with Thoracic Motions for Myocardial Perfusion Imaging

Yannis Parpottas[1,2], Sotiris Panagi[1,2], Costas Kyriacou[2], Demetris Kaolis[3], Ioannis Petrou[4]

[1]Frederick Research Center, Nicosia, Cyprus
[2]Frederick University, Nicosia, Cyprus
[3]Department of Medical Physics, State Health Services Organisation, Cyprus
[4]Department of Nuclear Medicine, Nicosia General Hospital, State Health Services Organisation, Cyprus

Introduction

Coronary artery disease (CAD) is the most common form of heart disease worldwide. Myocardial perfusion imaging (MPI) has been proven to be able to assess the functional significance of a coronary artery stenosis [1].

Thoracic motions may cause artifacts and false positive findings reducing the diagnostic accuracy on MPI [2]. Physical thoracic phantoms with motions, that can operate simultaneously or independently to each other, are useful to separately study the effect of each motion on physicians' MPI reports.

The purpose of this study was to validate the cardiac-lungs-liver cranio-caudal respiratory motion in an anthropomorphic phantom assembly. This motion is important to study the influence of MP artifacts, due to motion and liver activity, on physicians' MPI reports.

Materials & Methods

Phantom assembly

The phantom assembly consists of an anthropomorphic thorax phantom with thoracic moving phantoms (figure 1). The thorax encloses, in proper anatomical positions, human-sized and shaped thoracic phantoms of: (a) an ECG beating left ventricle (LV), (b) inflatable lungs, and (c) a liver. These thoracic phantoms can also oscillate in the cranio-caudal direction for different respiratory amplitudes. All thoracic motions can function simultaneously or independently to each other, and they are controlled by a Programmable Logic Controller (PLC).

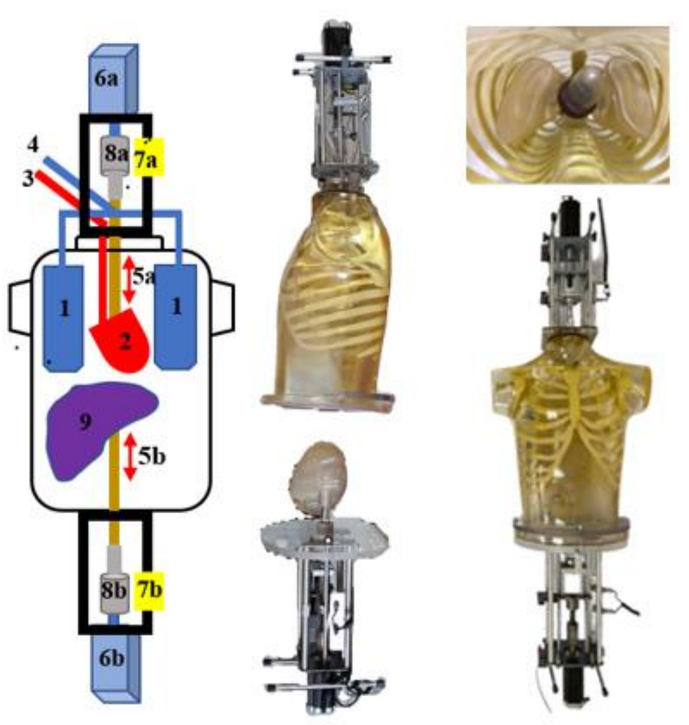

Figure 1. (Left) The design of the anthropomorphic thorax phantom with the enclosed **(1)** lungs, **(2)** cardiac, **(9)** liver phantoms, and with the attached mechanisms to support the cranio-caudal respiratory motions of the cardiac **(5-8a)** and liver **(5-8b)** phantoms, where **(5)** are the solid-water rods, **(6)** are the motors, **(7)** are the aluminium support frames, and **(8)** are the screwed stainless-steel rods. **(Middle)** Side-view of the anthropomorphic phantom with (a) the motion mechanism of the cardiac phantom, attached to the neck, and (b) the liver phantom and its motion mechanism, outside of the thorax, but attached to the thorax base. **(Top-right)** The cardiac and lungs phantoms within the thorax. **(Bottom-right)** The anthropomorphic phantom assembly with the enclosed thoracic phantoms and the attached motion mechanisms.

Continuous motion

The cardiac phantom of the left ventricle is based on an inner-outer membrane system. The inner membrane (42 mL) represents the left ventricle and the closed cavity between the inner and outer membrane (90 mL) represents the myocardial wall of the LV [3-7]. Diastole and systole can be achieved by pumping water into and out the inner membrane using a rotary motor and a piston, which follows the cardiovascular physiology described by the Wigger diagram. An ECG gating circuit synchronizes the LV beating with the SPECT modality to simulate the clinically gated acquisitions. In addition, cardiac defects of various sizes can be positioned, and radio-pharmaceuticals can be injected within the LV myocardial wall. The heart rate and ejection fraction can be controlled by the Programmable Logic Controller (PLC).

Each lung is covered with a thermoplastic structure, which forms the lung shape at end-inspiration, to allow inflation in all directions in a physiologically correct manner. The cavities within the lungs are filled with a lung-equivalent material. The respiratory pattern (sinusoidal exponential), the breath rate and the tidal volume are controlled by the PLC. In particular, the PLC controls two electro-proportional valves which regulated the pressure of the air, with respect to time, entering the lungs for inhalation and escaping from the lungs for exhalation, respectively [7]. In the PLC mode for normal respiration, the tidal volume is set to 450 mL, and the corresponding one for deep respiration is set to 550 mL. The initial volume of both lungs is 1100 mL.

During respiration, the cardiac and liver phantoms can oscillate in the cranio-caudal direction, in synchronization with the inferior portion of the inflatable lungs. In this motion, the cardiac phantom is controlled by (a) an actuator rod that enters in the thorax from the neck, (b) a linear motor and (c) the PLC. In the case of the liver phantom, a similar mechanical system controls the motion, but the actuator rod enters in the thorax from the thorax base (figure 1). In the PLC mode for normal respiration, the maximum oscillatory amplitude of the cardiac-liver phantom is set to 1.5 cm, and the corresponding one for the deep respiration is set to 2.7 cm.

The cardiac-liver proximity is regulated by the length of the liver's actuator rod that enters in the thorax. This proximity can be easily set to any value between 0.5 to 2 cm, at diastole, in distance intervals of 0.5 cm.

Static and dynamic respiratory phases

A PLC mode controls the static and another mode the dynamic respiratory phases. The respiration of the thoracic phantoms is divided into four static respiratory phases from end-exhalation (phase-1) to end-inhalation (phase-4). Each static phase is characterized with a specific air volume in the lungs and a specific cardiac-liver displacement towards the caudal direction. Dynamic respiratory phases can be performed between two successive static phases. Table 1 shows the values of the lungs' air volume and the cardiac-liver displacements, in each phase, in normal and deep respiration.

Table 1. Air volume of the lungs and cardiac-liver displacements, in each static phase, in normal and deep respiration; phase-1 is at end-exhalation and phase-4 is at end-inhalation.

		Normal Respiration		Deep Respiration	
Dynamic respiratory phase	Oscillation between static phases	Lungs' volume (ml)	Cardiac-liver displacement (mm)	Lungs' volume (ml)	Cardiac-liver displacement (mm)
1	1↔2	1100↔1145	0↔5	1100↔1155	0↔5
2	2↔3	1145↔1344	5↔10	1155↔1398	5↔20
3	3↔4	1344↔1550	10↔15	1398↔1650	20↔27

Validation procedure

The Toshiba Aquilion RXL 16-CT system of the Limassol General Hospital was utilized to perform CT acquisitions of the anthropomorphic phantom assembly. The slice thickness was 0.5 mm (1200 slices per image), the tube voltage was set at 120 kV_p and the current at 100 mA.

The OsiriX software was used to measure and validate the various cardiac-liver proximities and the values of Table 1.

Results

Figure 2 shows the coronal CT slices of the anthropomorphic phantom assembly with the cardiac phantom at systole (left) and at diastole (right). The cardiac-liver proximity at diastole was set and measured to be 0.5 cm, and consequently, at systole was measured to be 1.5(1) cm, since the beating cardiac phantom contracts by about 1 cm. The same measurement was repeated for all cardiac-liver proximities that the phantom assembly is capable to have. Mechanically, this proximity is controlled by a laser sensor with an error of 1 mm.

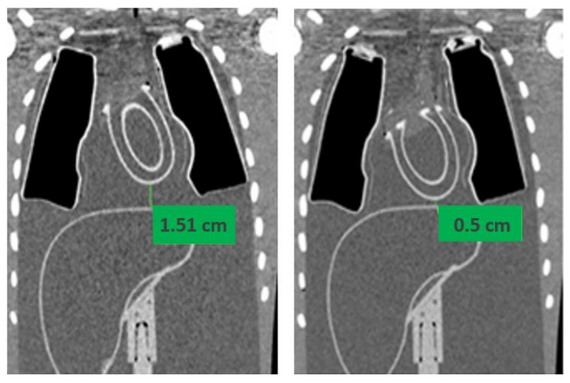

Figure 2. Coronal CT slices of the anthropomorphic phantom assembly for a cardiac-liver proximity of 0.5 cm at diastole (right), and consequently 1.5 cm at systole (left).

Figure 3 shows the coronal (top row), sagittal (middle row) and axial (bottom row) slices of the anthropomorphic phantom assembly for the four static phases in deep respiration: phase-1 (1st column), phase-2 (2nd column), phase-3 (3rd column) and phase-4 (4th column). The displacement towards the caudal direction is indicated with the red lines. The increase of the air volume in the lungs is also shown. The liver-cardiac proximity was set to 0.5 cm at diastole. The volume of the lungs and the displacement of the cardiac-liver phantoms were measured, with the OsiriX software, to agree with the values of Table 1.

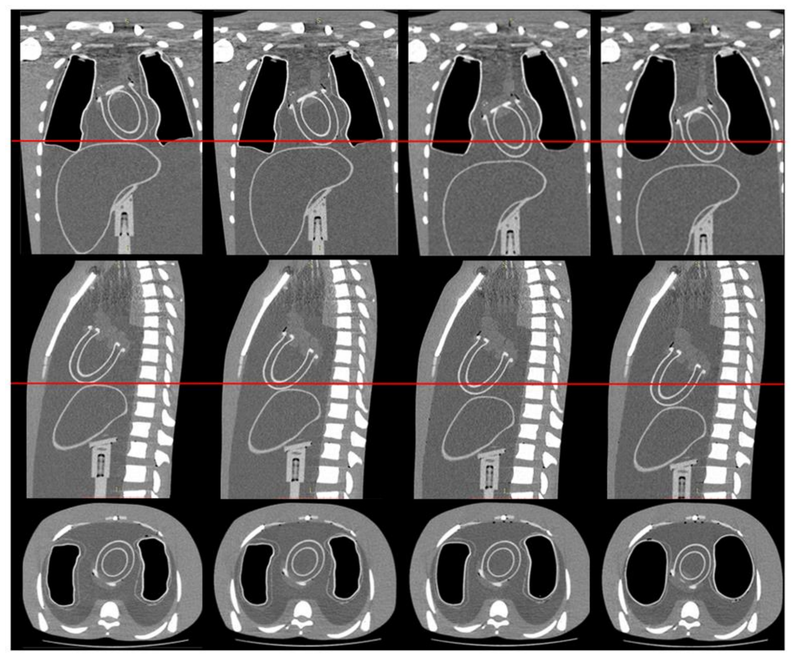

Figure 3. Coronal (top row), sagittal (middle row) and axial (bottom row) slices of the anthropomorphic phantom assembly for the four static phases (phase 1-to-4 from left-to-right columns, respectively) in deep respiration, according to the values of Table 1.

Conclusions

The addition of a liver compartment in the existing anthropomorphic phantom assembly and its synchronization with the existing motions will be useful to investigate MPI under the influence of different cardiac-liver activity ratios, different cardiac-liver proximities and different respiratory amplitudes.

Acknowledgements

This work was co-funded by the European Regional Development Fund and the Republic of Cyprus through the Research and Innovation Foundation (Project: EXCELLENCE /1216/0085).

References

1. Baghdasarian SB and Heller GV. The role of myocardial perfusion imaging in the diagnosis of patients with coronary artery disease: Developments over the past year. Curr Opin Cardiol 2005; 20:369-74.
2. Wheat JM and Currie GM. Impact of patient motion on myocardial perfusion SPECT diagnostic integrity: Part 2. J Nucl Med Technol 2004; 32:158-63.
3. Chrysanthou-Baustert I, Parpottas Y, Demetriadou O, Christofides S, Yiannakkaras Ch, Kaolis D, et al. Diagnostic sensitivity of SPECT myocardial perfusion imaging using a pumping cardiac phantom with inserted variable defects. J Nucl Cardiol 2013; 20:609-15.
4. Chrysanthou-Baustert I, Polycarpou I, Demetriadou O, Livieratos L, Lontos A, Parpottas Y, et al. Characterization of attenuation and respiratory motion artifacts and their influence on SPECT MP Image evaluation using a dynamic phantom assembly with variable cardiac defects. J Nucl Cardiol 2017; 24(2):698-707.
5. Polycarpou I, Chrysanthou-Baustert I, Demetriadou O, Parpottas Y, Panagidis C, Marsden KP, et al. Impact of respiratory motion correction on SPECT myocardial perfusion imaging using a mechanically moving phantom assembly with variable cardiac defects. J Nucl Cardiol 2017; 24(4):1216-25.
6. Lontos A, Antoniou A, Chrysanthou-Baustert I, Christofides S, Demetriadou O, Parpottas Y, et al. Construction of Inflatable Lungs to Simulate Respiratory Motion in Myocardial Perfusion Imaging. In: XIV Mediterranean Conference on Medical and Biological Engineering and Computing, IFMBE Proceedings 2016; 57:1337-41.
7. Panagi S, Antoniou A, Chrysanthou-Baustert I, Kaolis D, Demetriadou O, Kyriacou C and Parpottas Y. Controlled Thoracic Motions of an Anthropomorphic Phantom for Myocardial Perfusion Imaging, In: XV Mediterranean Conference on Medical and Biological Engineering and Computing, IFMBE Proceedings 2020; 76:727–34.